Study of VBF Higgs via Di-photon Decay at ATLAS

Yaquan Fang (方亚泉)
Institute of High Energy Physics, Beijing

22-25 August, 2022

Multi-Boson Interactions 2022

School of Physics and Astronomy, Shanghai Jiao Tong University

Introduction

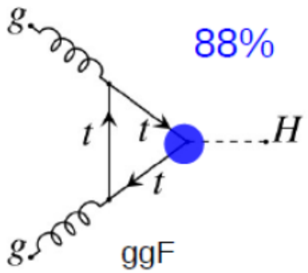

Gluon-gluon fusion

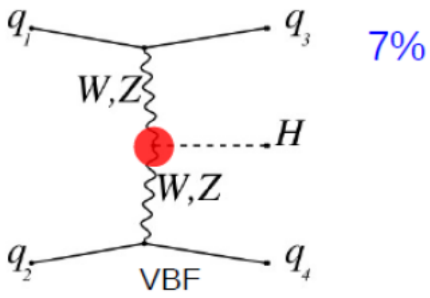

Vector Boson Fusion (VBF)

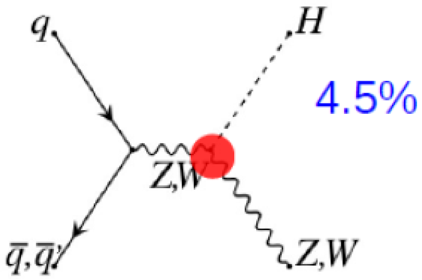

W/ZH

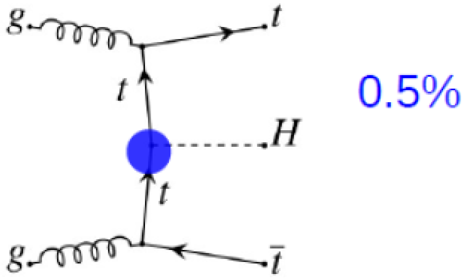

ttH

- After the Higgs discovery, it is important to study the Higgs property according to its production, decays, coupling, spin
- VBF provides us an opportunity to understand:
    - Higgs production mode
    - Electro-weak production
    - Search for new physics

Contribution of VBF $\mathbf{H} \rightarrow \gamma\gamma$ to Higgs Discovery in ATLAS

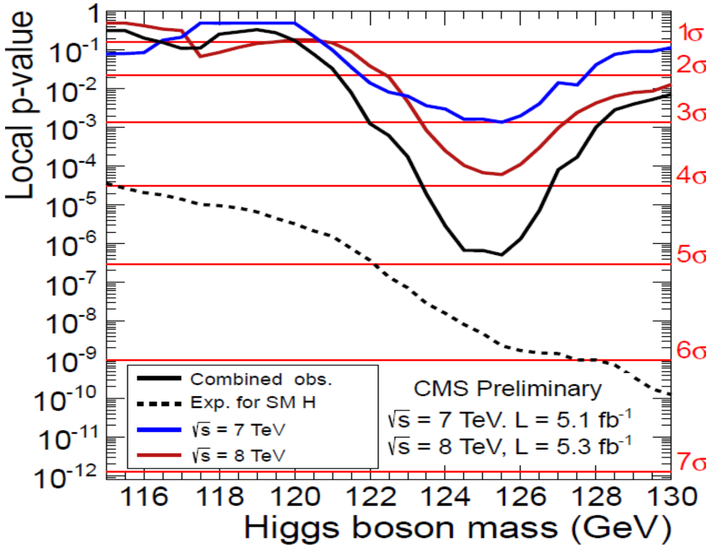

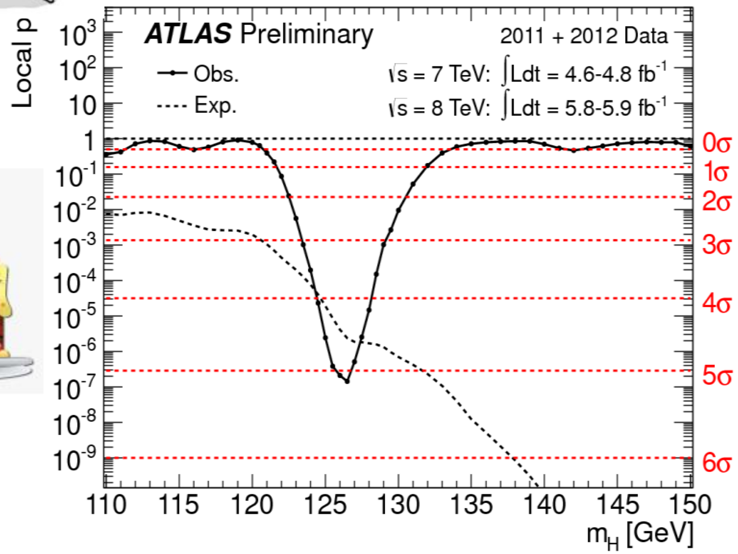

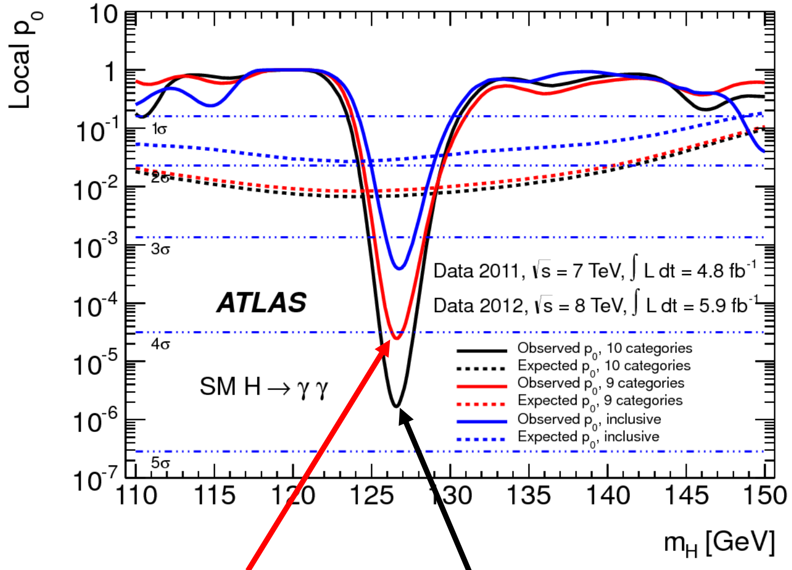

Without VBF cat: 4.0σ

With VBF cat. : 4.4σ

- ➢Higgs boson discovered 10 years ago shows that SM is a successful one in particle physics.
- ➢Higgs boson is crucial to give mass to other particles.
- ➢VBF H→ $\gamma\gamma$ played an important role in the Higgs discovery in ATLAS.

A Candidate of VBF Higgs Event Decaying into Two Photons

VBF tagged jets

Higgs Decay

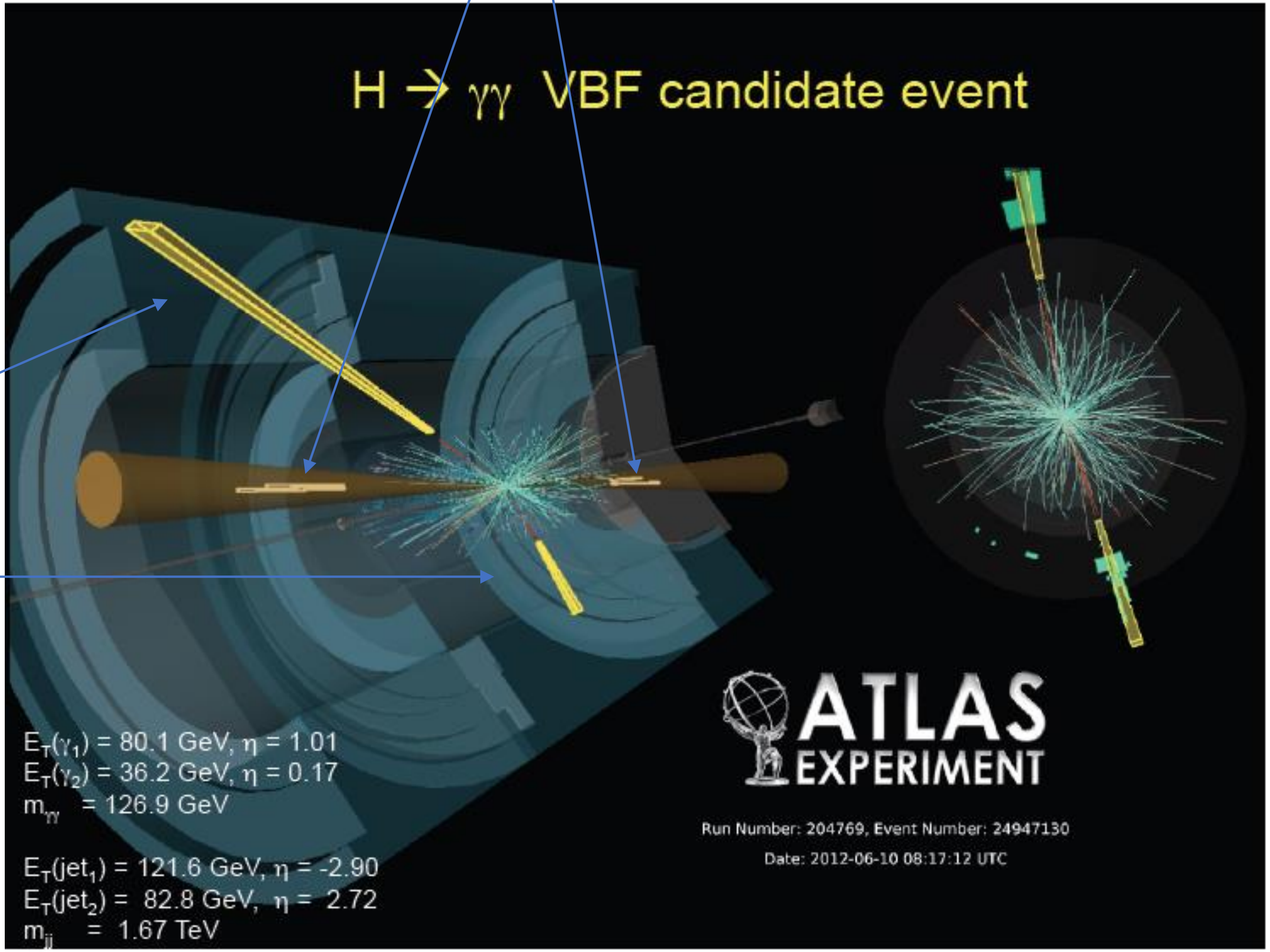

Event Signature of VBF Higgs

- Two forward highly boosted jets.
  - High invariant mass of the di-jet (M_{jj}) and rapidity gap between the two jets ($\Delta\eta_{jj}$)
- The jet activities are suppressed between two VBF jets.
  - Central jet veto
- Multivariate analyses (MVA) to improve the sensitivities.

Wisconsin Pheno. Group:
T. Han, D.L. Rainwater, D. Zeppenfeld et al.

Central jet veto initially suggested in PRD 42 3052 (1990)

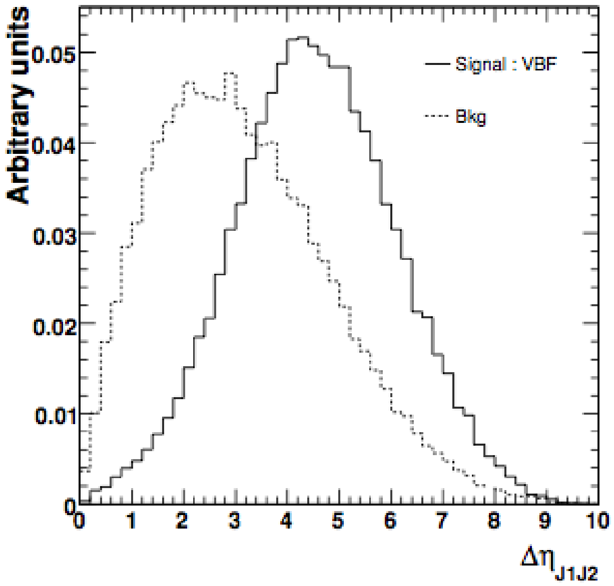

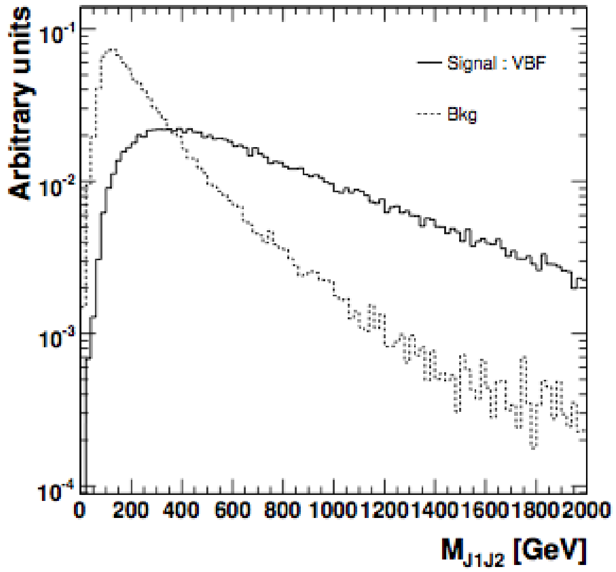

Example: discriminating variables used in ATLAS for H→γγ analysis

- 6 variables below used to separate signal from background

Variables	Definition	Separation power
m_{jj}	Invariant mass of dijet	0.256
$\Delta\eta_{jj}$	Pseudo-rapidity separation of dijet	0.130
$\Delta\Phi_{\gamma\gamma,jj}$	Azimuthal angle between diphoton and dijet system	0.199
p_{Tt}	Diphoton p_T projected perpendicular to the diphoton thrust axis	0.235
$\Delta R^{min}_{\gamma,j}$	Minimum ΔR between one of the two leading photons and the corresponding leading jets	0.185
$\eta^{Zeppenfeld}$	$\lvert\eta_{\gamma\gamma} - 0.5 * (\eta_{j1} + \eta_{j2})\rvert$	0.126

- Separation power: $$< S^2 >= \frac{1}{2}\int \frac{(\hat{y}_s(y) - \hat{y}_b(y))^2}{\hat{y}_s(y) + \hat{y}_b(y)} dy$$
  - two forward jet → large $\Delta\eta_{jj}$
  - high p_T and large $\Delta\eta_{jj}$ jets → large m_{jj}
  - central diphoton and forward dijet → large $\Delta R^{min}_{\gamma,j}$, low η^{Zepp}
  - two photons balancing high p_T jets → high p_{Tt}

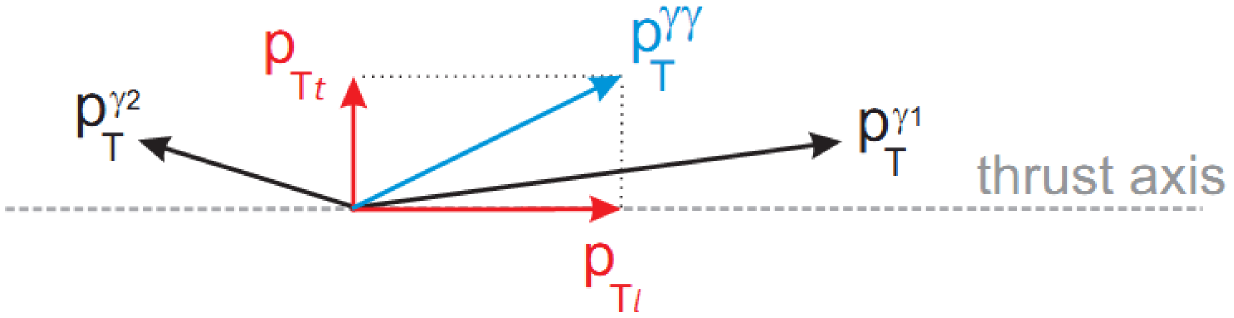

Distributions of the discriminating variables

Phys.Rev. D 98 (2018) 052005

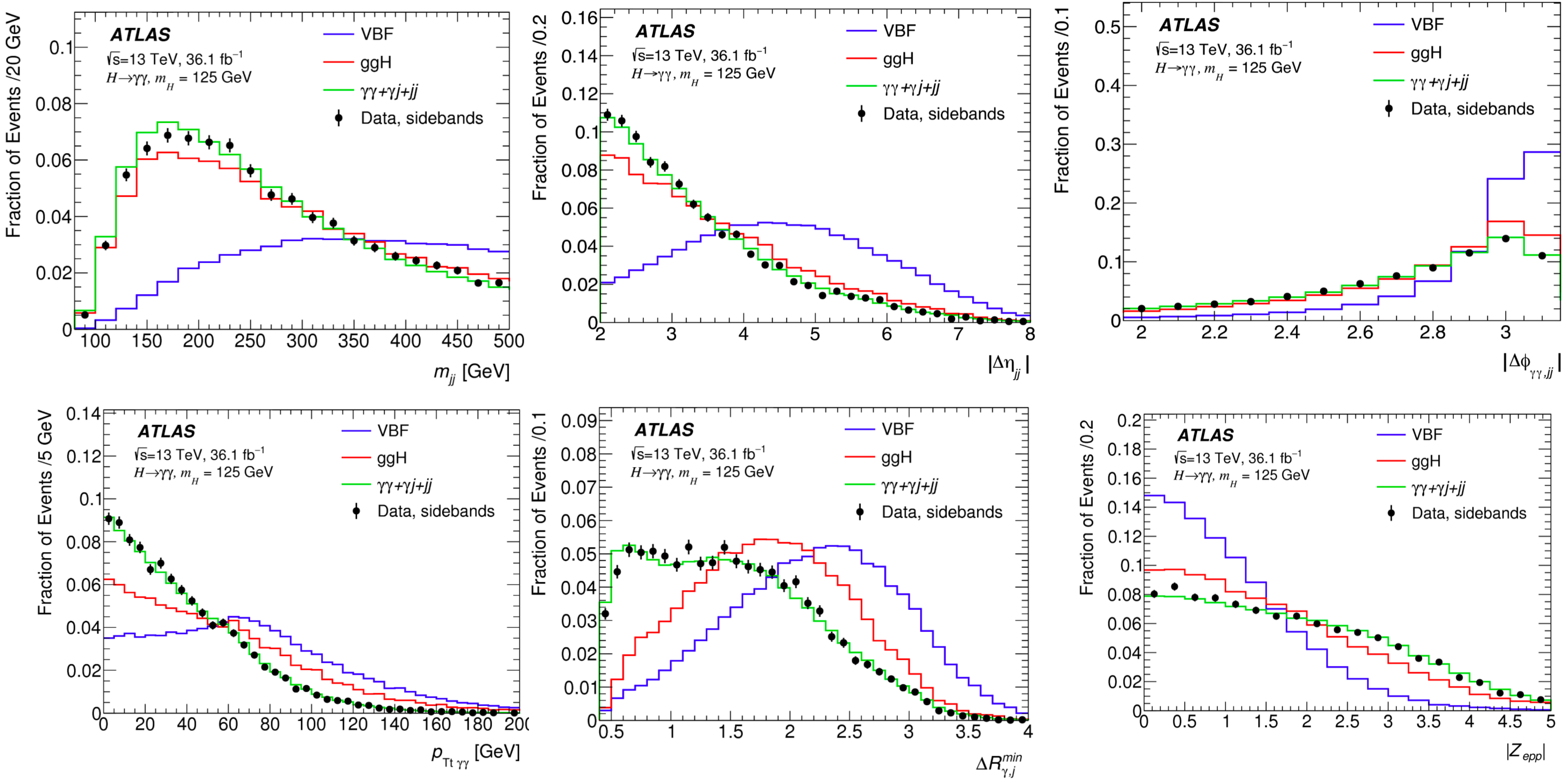

MVA method: Training/optimization

- [120,130] GeV $m_{\gamma\gamma}$ window for data is blinded for training and optimization.
- Signal : VBF 125 GeV.
- Background :
  - $\gamma\gamma$: SHERPA Monte-Carlo .
  - γjet+jets : data with at least one not isolated photon (revIso).
  - The fraction of the two components above are obtained from data-driven method.
  - Overall contribution is normalized to the data.
- For the optimization, both sideband fit from data and MC+revIso are tested
- Divide events into 1-2 categories according to BDT scores; The improvement is above 10-20% w.r.t cut based one.

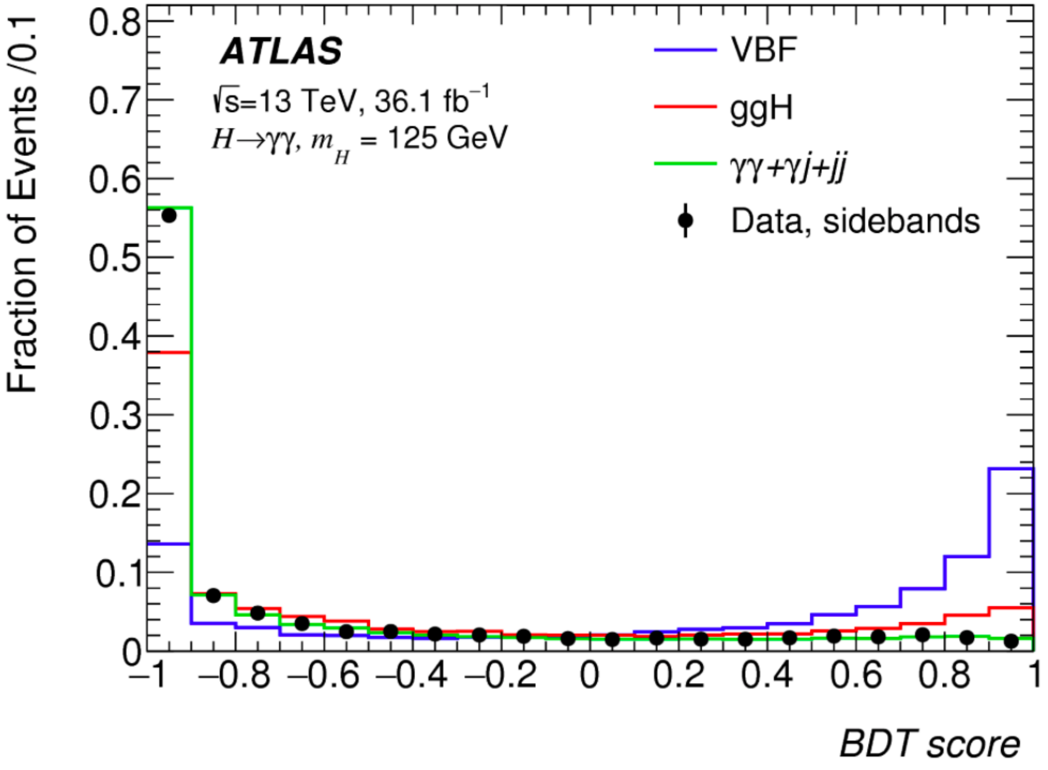

ATLAS RUN2 VBF H→γγ results (36.1 fb^{-1})

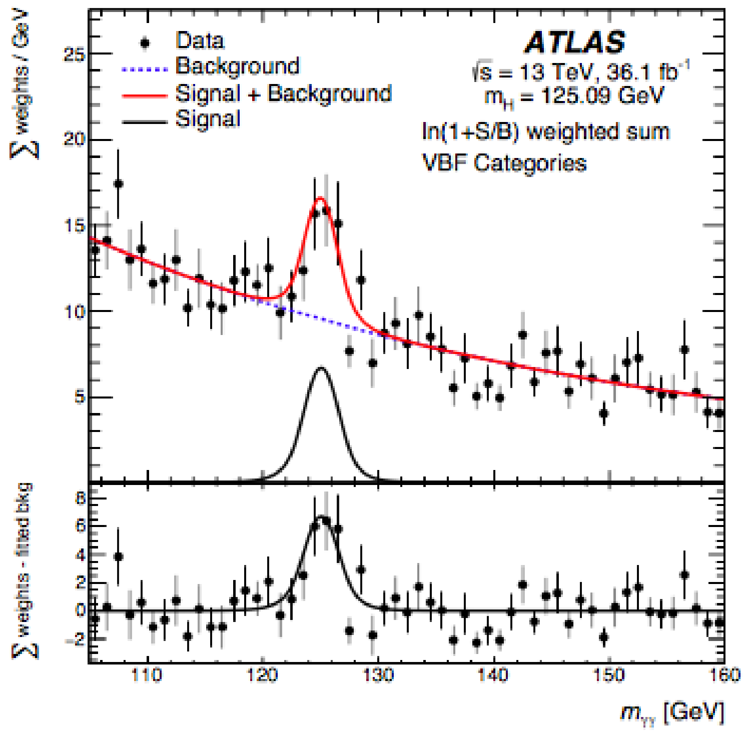

Measurement	Exp. Z_0	Obs. Z_0
μ_{VBF}	$2.6\ \sigma$	$4.9\ \sigma$
μ_{VH}	$1.4\ \sigma$	$0.8\ \sigma$
μ_{top}	$1.8\ \sigma$	$1.0\ \sigma$

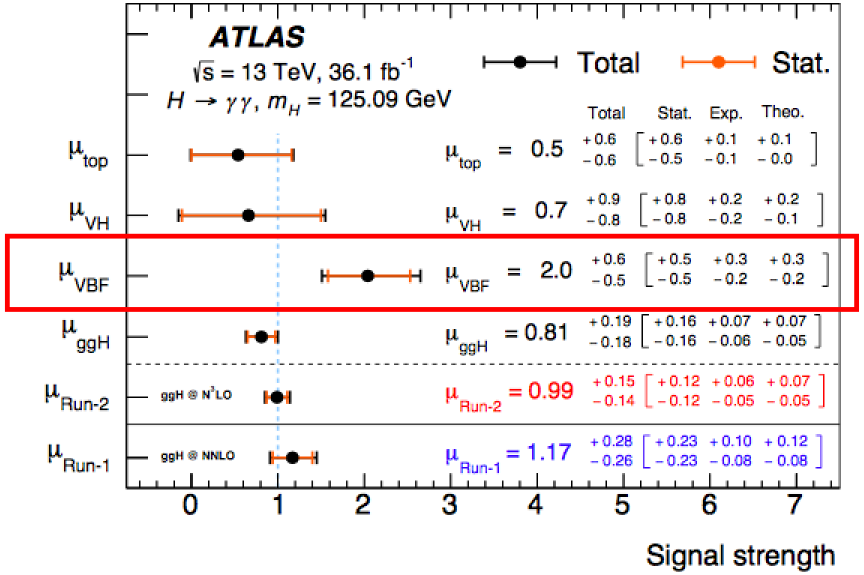

- 4.9σ observed with 2.6σ expected from single experiment.
- The signal strength is ~2xSM, which is still consistent with SM prediction within uncertainties.
- Published at Phys. Rev. D 98, 052005 (2018)

RUN2 VBF H→γγ results (79.8 fb^{-1})

ATLAS-CONF-2018-028

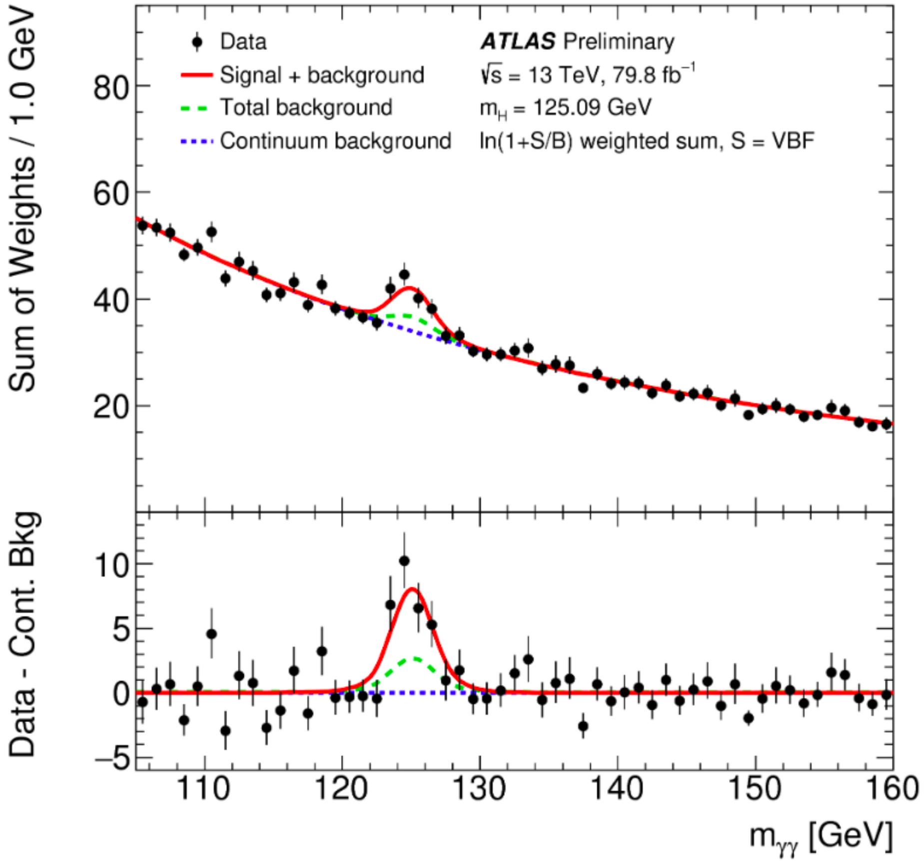

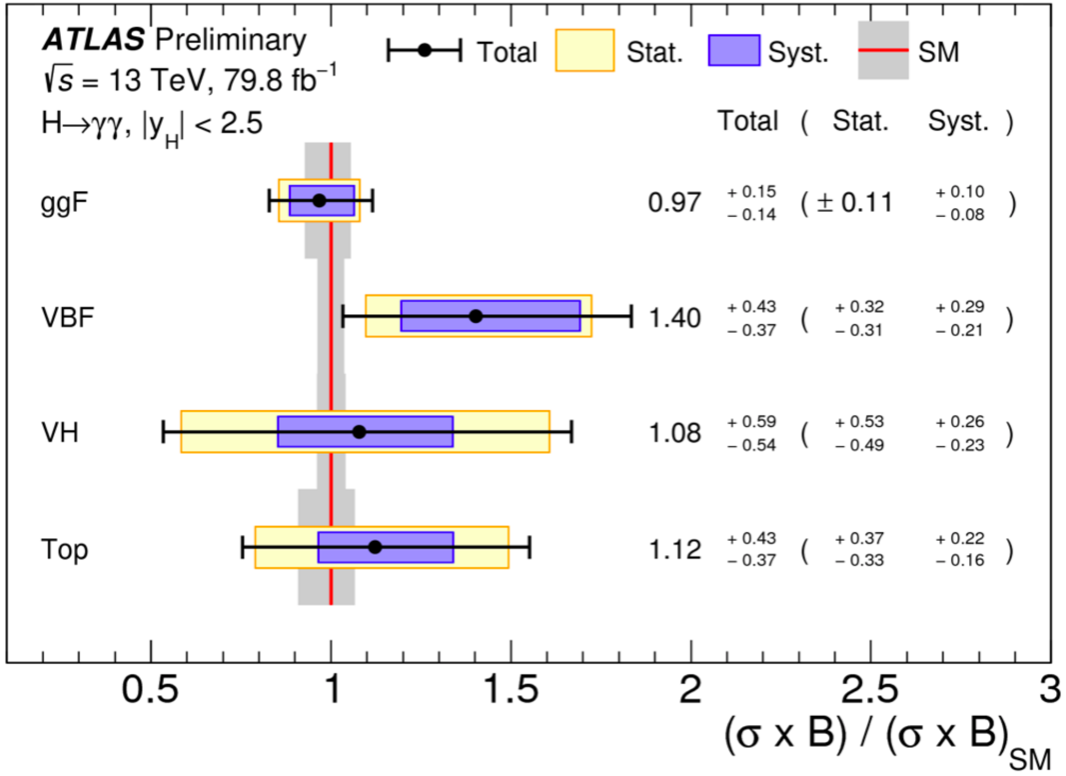

- The signal strength is well consistent with SM prediction within uncertainties

Combination of different channels

ATLAS-CONF-2018-031

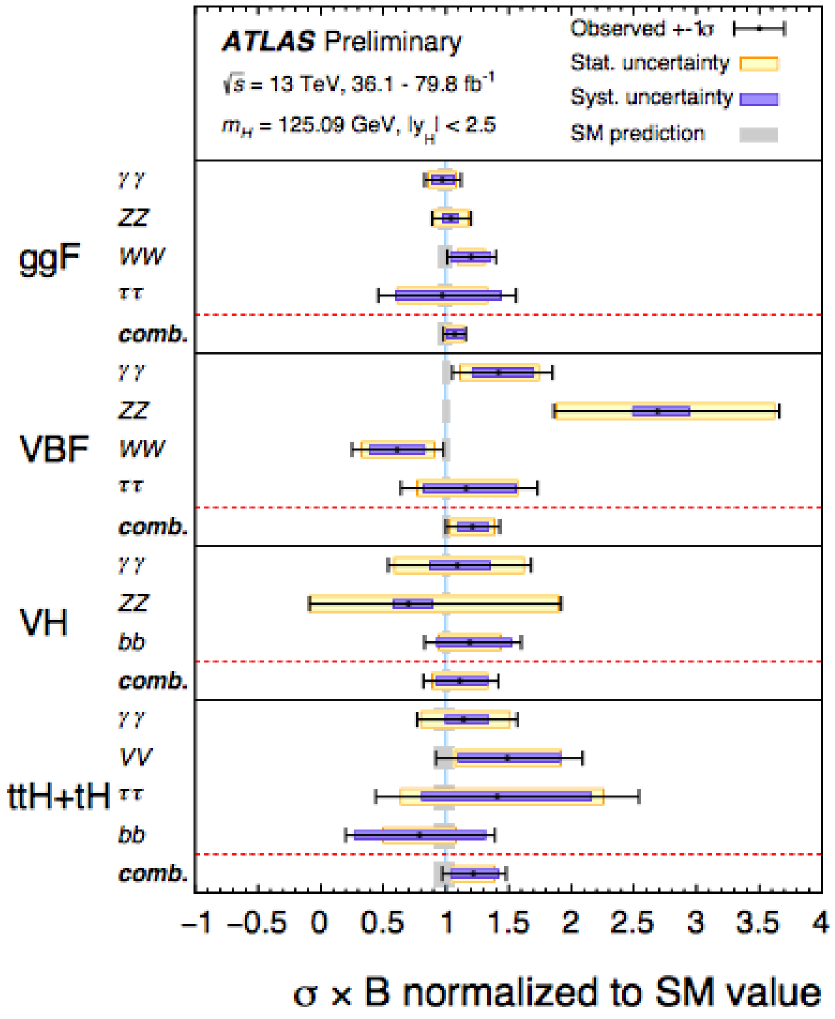

Process ($\|y_H\| < 2.5$)	Value [pb]	Uncertainty [pb] Total	Stat.	Exp.	Sig. th.	Bkg. th.	SM pred. [pb]	Significance obs. (exp.)
ggF	47.8	± 4.0	± 3.1	$^{+2.7}_{-2.2}$	± 0.9	± 1.3	44.7 ± 2.2	-
VBF	4.25	$^{+0.77}_{-0.74}$	± 0.63	$^{+0.39}_{-0.35}$	$^{+0.25}_{-0.21}$	$^{+0.14}_{-0.11}$	3.515 ± 0.075	6.5 (5.3)
WH	1.89	$^{+0.63}_{-0.58}$	$^{+0.45}_{-0.42}$	$^{+0.29}_{-0.28}$	$^{+0.25}_{-0.16}$	$^{+0.23}_{-0.22}$	1.204 ± 0.024	4.1 (3.7)
ZH	0.59	$^{+0.33}_{-0.32}$	$^{+0.27}_{-0.25}$	± 0.14	$^{+0.08}_{-0.02}$	± 0.11	$0.794^{+0.033}_{-0.027}$	
$t\bar{t}H+tH$	0.71	± 0.15	± 0.10	± 0.07	$^{+0.05}_{-0.04}$	$^{+0.08}_{-0.07}$	$0.586^{+0.034}_{-0.050}$	5.8 (5.3)

- Combining H→γγ, *ZZ**,*WW**, one can achieve 6.5σ (5.3σ) observed (expected) for VBF Higgs.
- The dominant contribution is from H→γγ.
- The result is well consistent with SM prediction.

Run2 VBF H→γγ results (139 fb^{-1})

arXiv: 2208.02338

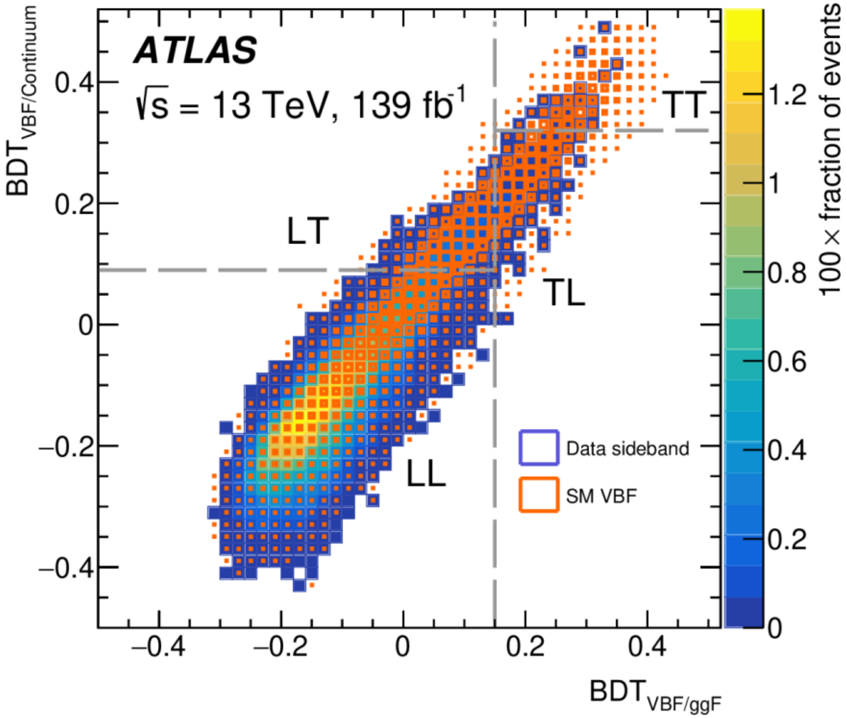

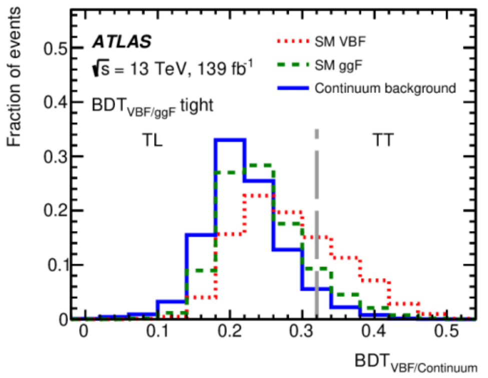

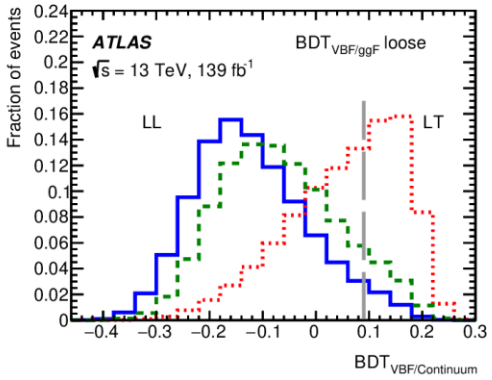

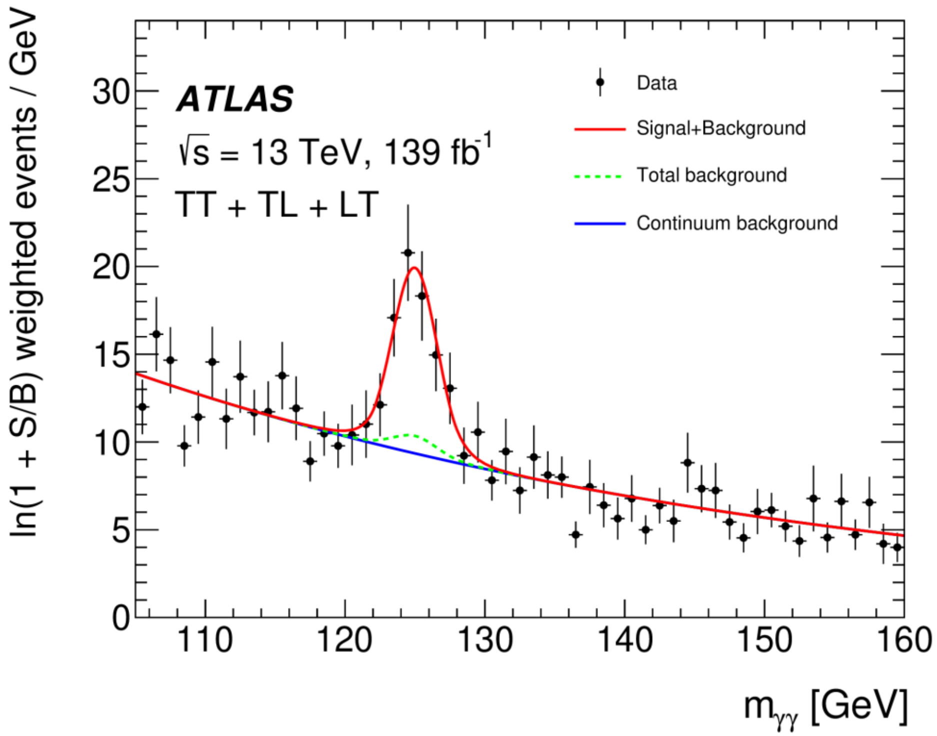

Two dedicated BDTs are developed to suppress both continuum bkg and ggFusion Higgs.

CP Properties study via VBF H→ $\gamma\gamma$

arXiv: 2208.02338

- **Motivation**
  - ✓ Study the CP structure of interactions between the Higgs boson and EWK gauge bosons

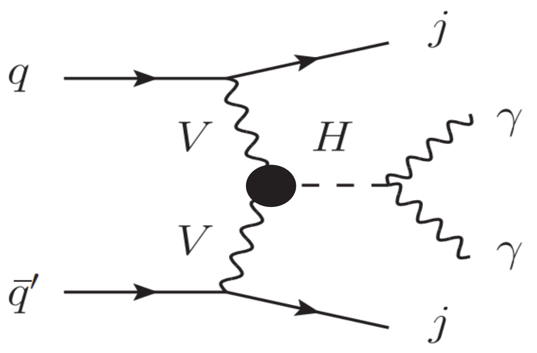

- **Explored two EFT bases**
  - ✓ HISZ basis
    - After EWSB, EFT Lagrangian can be written as

$$\mathcal{L}_{\text{eff}} = \mathcal{L}_{\text{SM}} + \tilde{g}_{H\gamma\gamma} H \tilde{A}_{\mu\nu} A^{\mu\nu} + \tilde{g}_{H\gamma Z} H \tilde{A}_{\mu\nu} Z^{\mu\nu} + \tilde{g}_{HZZ} H \tilde{Z}_{\mu\nu} Z^{\mu\nu} + \tilde{g}_{HWW} H \tilde{W}^{+}_{\mu\nu} W^{-\mu\nu}$$

    - Dimensionless parameters introduced: d and $\tilde{d}$, with assuming $d = \tilde{d}$

$$\tilde{g}_{H\gamma\gamma} = \tilde{g}_{HZZ} = \frac{1}{2}\tilde{g}_{HWW} = \frac{g}{2m_W}\tilde{d} \quad \text{and} \quad \tilde{g}_{H\gamma Z} = 0 . \qquad \mathcal{M} = \mathcal{M}_{SM} + \tilde{d} \cdot \mathcal{M}_{CP-odd} .$$

  - ✓ Warsaw basis

$$\mathcal{L}^{\text{CP-odd}}_{\text{SMEFT}} \supset \frac{c_{H\tilde{W}}}{\Lambda^2} H^\dagger H W^I_{\mu\nu} W^{\mu\nu I} + \frac{c_{H\tilde{B}}}{\Lambda^2} H^\dagger H B^A_{\mu\nu} B^{\mu\nu} + \frac{c_{H\tilde{W}B}}{\Lambda^2} H^\dagger \sigma^I H W^I_{\mu\nu} B^{\mu\nu}$$

    - VBF production is dominated by HWW vertex, analysis mainly explores $c_{H\tilde{W}}$

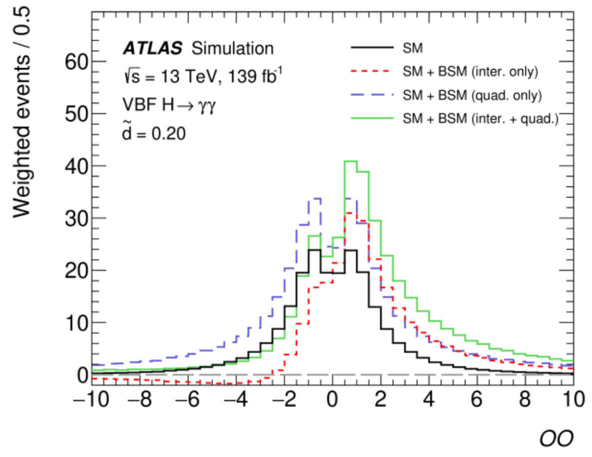

- **CP sensitive variable**
  - ✓ Optimal Observable
  - ✓ Inputs to Hawk: the 4-momentum of Higgs, two forward jets

$$OO = \frac{2Re(\mathcal{M}^*_{SM}\mathcal{M}_{CP-odd})}{|\mathcal{M}_{SM}|^2}$$

Analysis Strategies

Separate VBF from bkgs:
- ✓ Use $m_{\gamma\gamma}$ as a discriminator
  - ✓ DSCB for VBF/ggF
  - ✓ 2^{nd} Pol. for continuum bkg.
- ✓ 2 BDTs : VBF/cont. & VBF/ggF
  - ✓ Divide into 3 regions
  - ✓ 6 variables on page 7

Compute OO for :
- ✓ 3 (TT,TL,LT cats) x 6 (OO bins)
  - ✓ Compute OO for each data event
- ✓ Compute OO w/ various $\tilde{d}$ hypotheses
  - ✓ OO distribution for SM VBF is symmetrical.

Implementation of the stat. test :
- ✓ Test diff. $\tilde{d}$ or $C_{H\tilde{W}}$
  - ✓ In practice, 18-bin simultaneous fit
- ✓ Majority of sensitivities from high OO bins (middle plot)

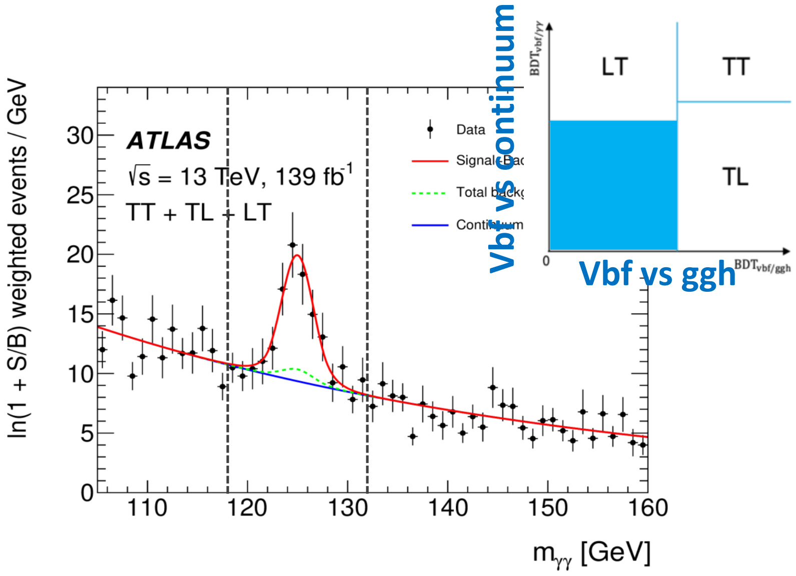

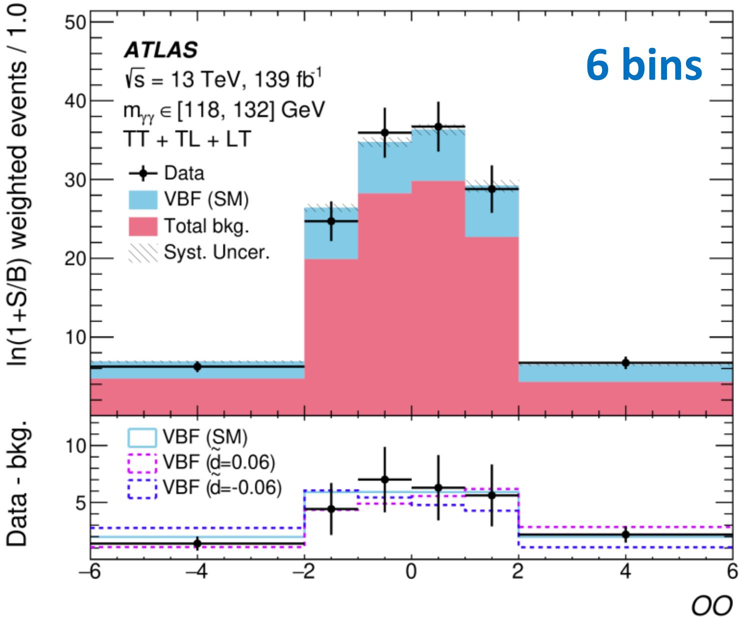

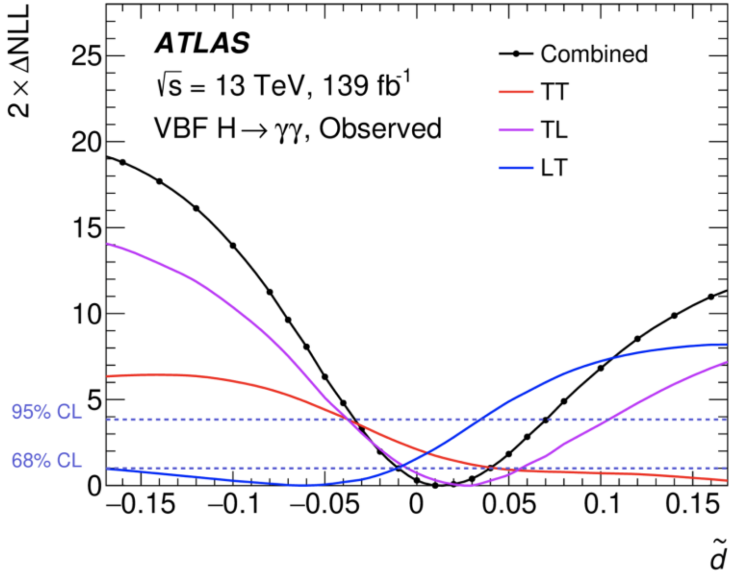

Results

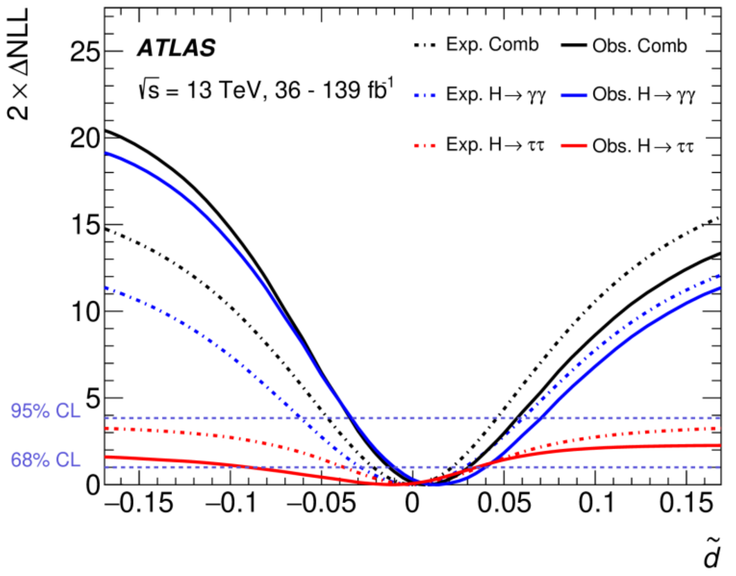

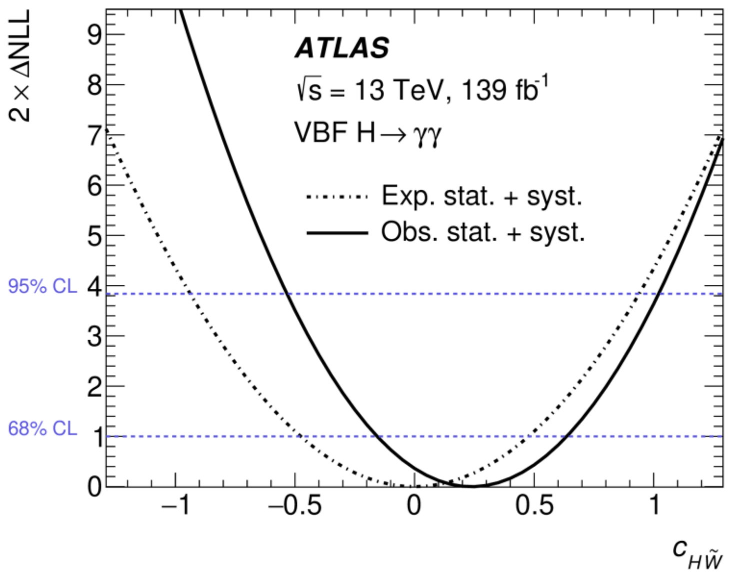

	68% (exp.)	95% (exp.)	68% (obs.)	95% (obs.)
$\tilde{d}$ (inter. only)	[−0.027, 0.027]	[−0.055, 0.055]	[−0.011, 0.036]	[−0.032, 0.059]
$\tilde{d}$ (inter.+quad.)	[−0.028, 0.028]	[−0.061, 0.060]	[−0.010, 0.040]	[−0.034, 0.071]
$\tilde{d}$ from $H \to \tau\tau$	[−0.038, 0.036]	–	[−0.090, 0.035]	-
Combined $\tilde{d}$	[−0.022, 0.021]	[−0.046, 0.045]	[−0.012, 0.030]	[−0.034, 0.057]
$c_{H\tilde{W}}$ (inter. only)	[−0.48, 0.48]	[−0.94, 0.94]	[−0.16, 0.64]	[−0.53, 1.02]
$c_{H\tilde{W}}$ (inter.+quad.)	[−0.48, 0.48]	[−0.95, 0.95]	[−0.15, 0.67]	[−0.55, 1.07]

- No CP violation is observed.
- Result for $\tilde{d}$ is further combined with $H \to \tau\tau$ analysis.
- Set most stringent constraints on CP-violation effect in HVV coupling

Comparisons with other Results

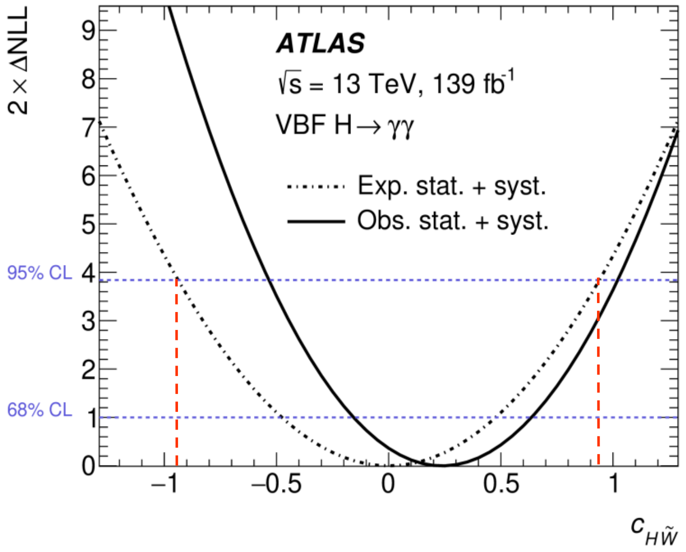

~5 times better constraint

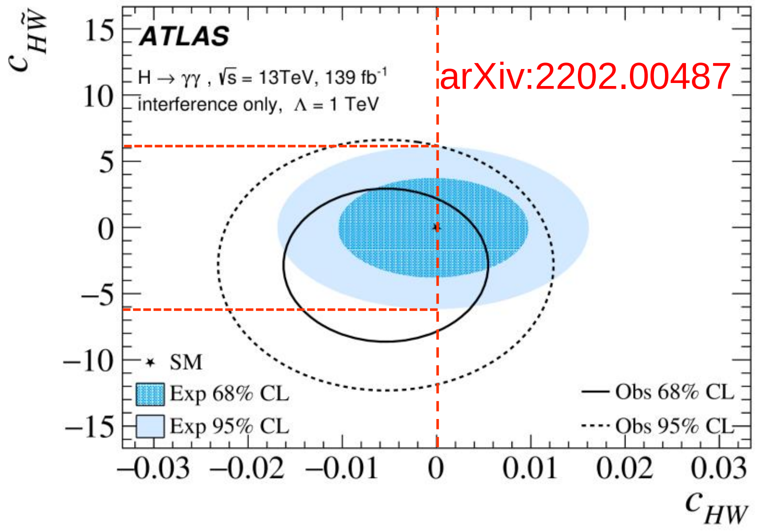

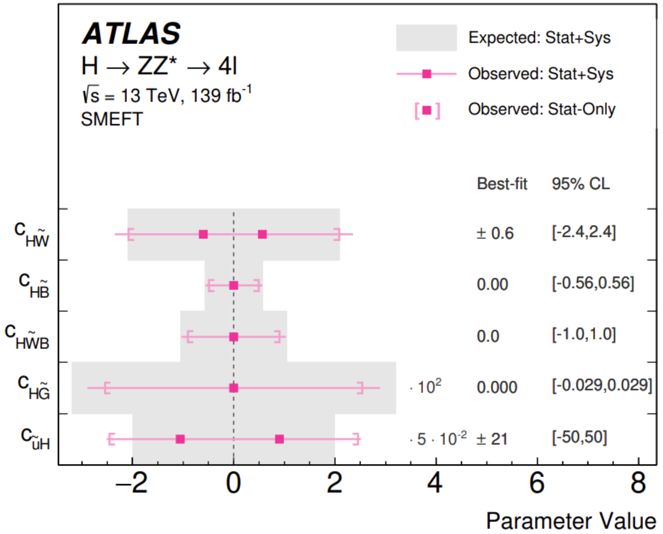

Channels	Coupling	Observed	Expected
Phys. Rev. D 104, 052004 (2021) **CMS** VBF & VH & H → 4ℓ	$c_{H\Box}$	$0.04^{+0.43}_{-0.45}$	$0.00^{+0.75}_{-0.93}$
	c_{HD}	$-0.73^{+0.97}_{-4.21}$	$0.00^{+1.06}_{-4.60}$
	c_{HW}	$0.01^{+0.18}_{-0.17}$	$0.00^{+0.39}_{-0.28}$
	c_{HWB}	$0.01^{+0.20}_{-0.18}$	$0.00^{+0.42}_{-0.31}$
	c_{HB}	$0.00^{+0.05}_{-0.05}$	$0.00^{+0.03}_{-0.08}$
68% constraints	$c_{H\tilde{W}}$	$-0.23^{+0.51}_{-0.52}$	$0.00^{+1.11}_{-1.11}$
	$c_{H\tilde{W}B}$	$-0.25^{+0.56}_{-0.57}$	$0.00^{+1.21}_{-1.21}$
	$c_{H\tilde{B}}$	$-0.06^{+0.15}_{-0.16}$	$0.00^{+0.33}_{-0.33}$

~2 times better constraint

Summary of the 10-Year Path ：
Study of VBF H→ $\gamma\gamma$

路漫漫其修远兮，吾将上下而求索

The road ahead will be long and our climb will be steep

Observation of VBF H

Contribution to Higgs discovery in ATLAS

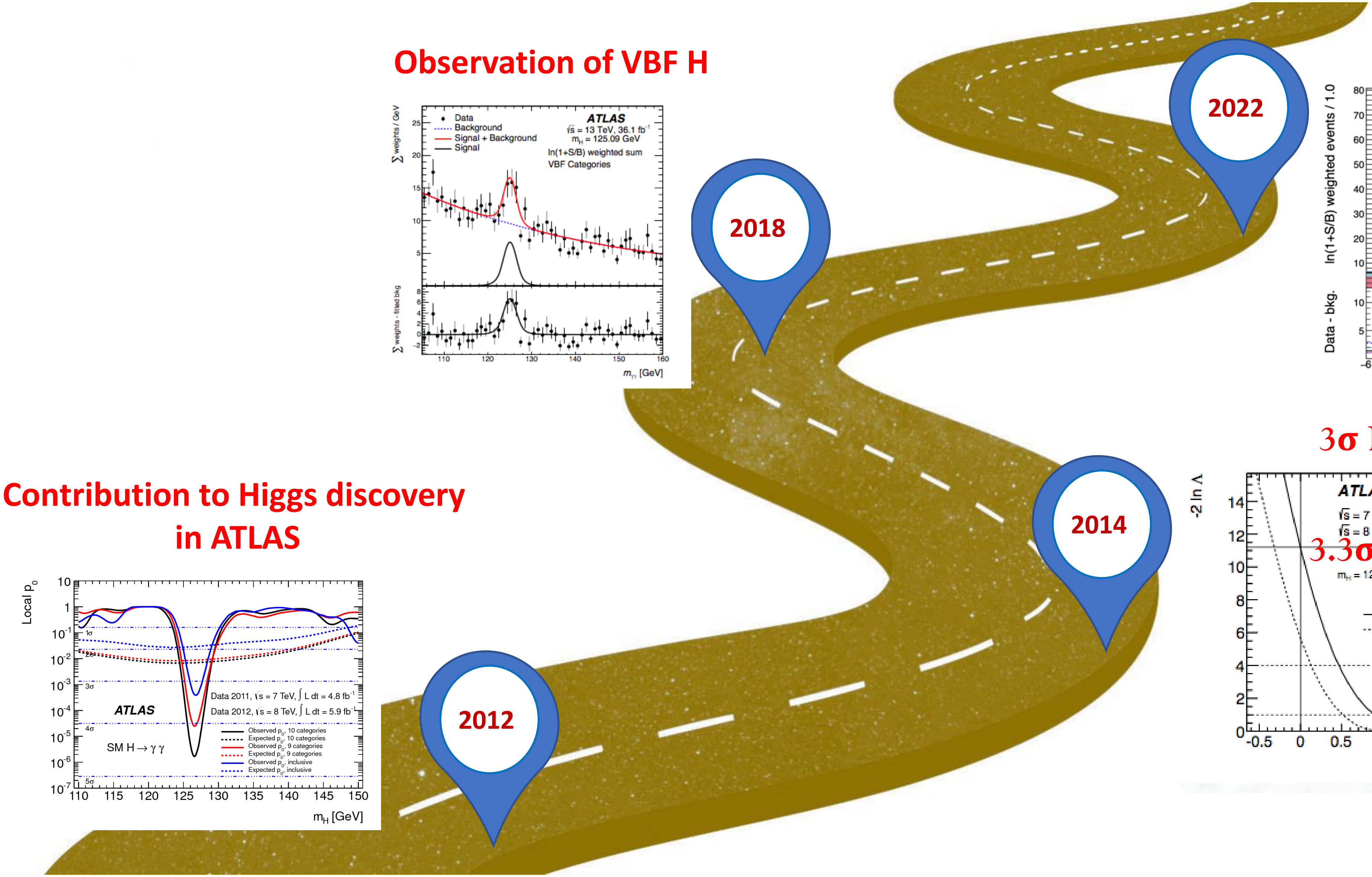

No CPV observed

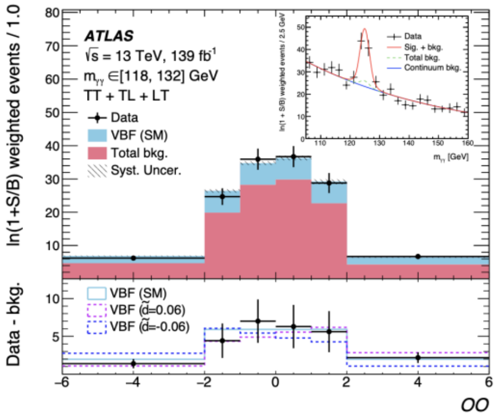

3σ Evidence

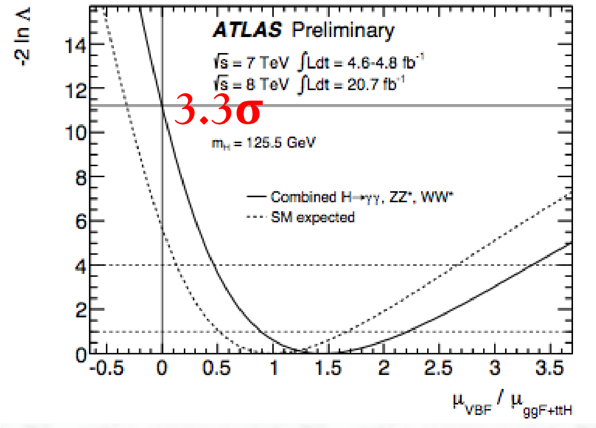

Conclusion

- VBF Higgs production has a unique event signature and have been intensively studied with MVA method.
- Results from the channels ($H\rightarrow ZZ^*, WW^*, \tau\tau, bb$) have been shown with 36.1,79.8 fb^{-1} data:
  - The combined result achieves 6.5σ/5.3σ (observed/expected), which is the first observation of VBF Higgs from single experiment.
  - $H\rightarrow\gamma\gamma$ makes a leading contribution.
- With full Run2 data, the CPV for $H\rightarrow\gamma\gamma$ with have been investigated
  - No BSM observed.
  - Provide the best limits

backup slides

VBF H→ZZ*

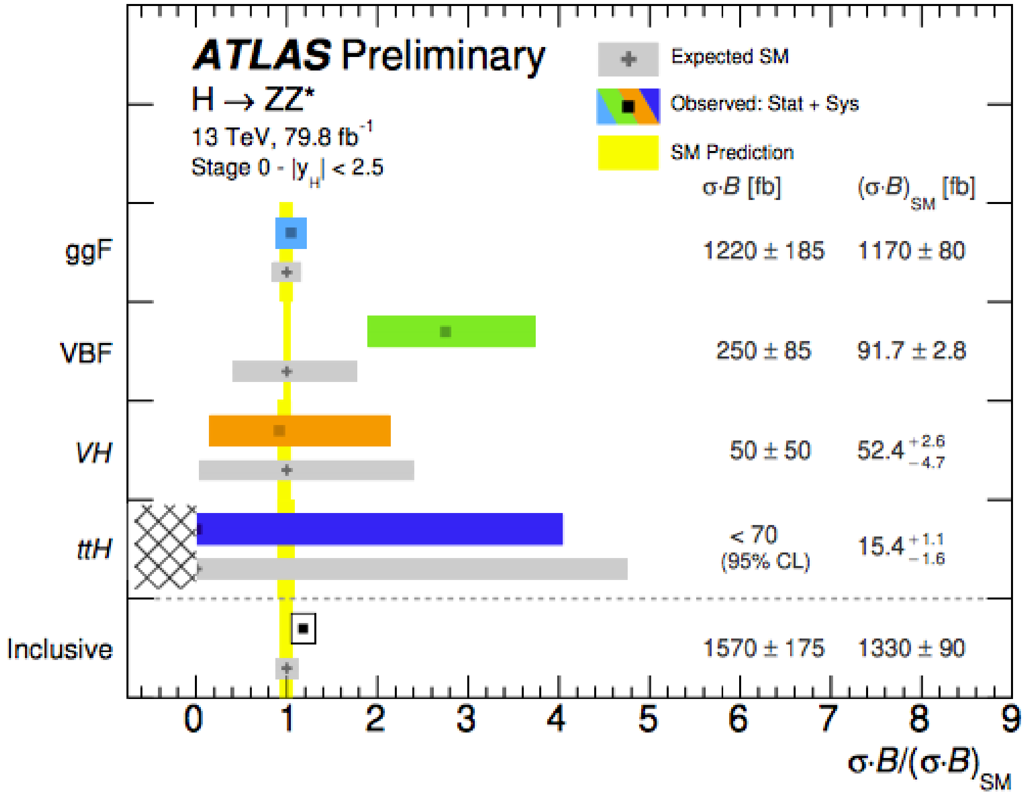

ATLAS-CONF-2018-018

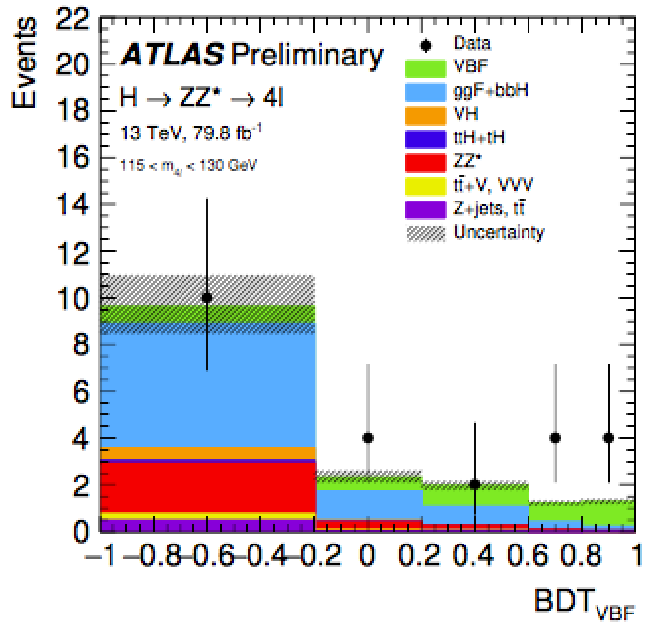

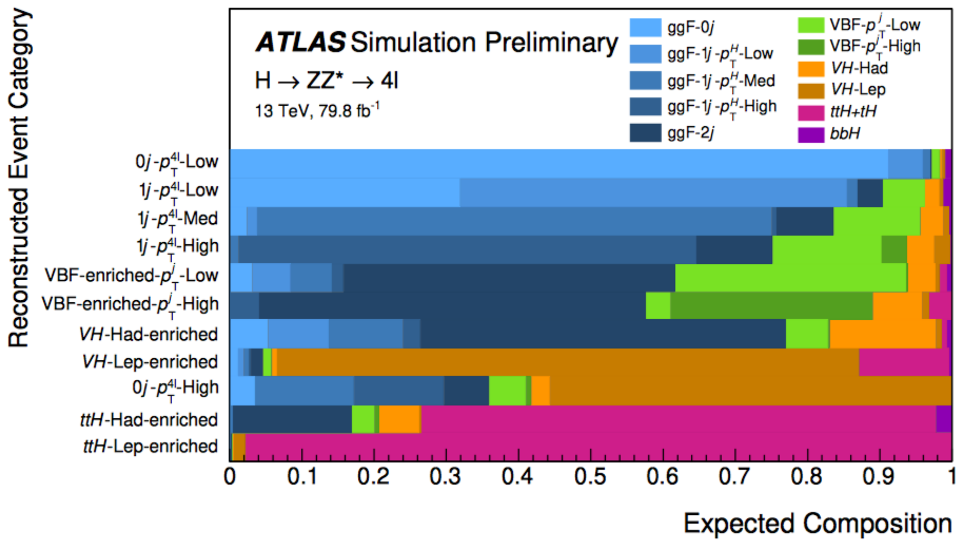

- ATLAS VBF H→*ZZ** is around 2.5xSM prediction which is still consistent with SM prediction considering the large statistical uncertainty
- Statistical uncertainty is the dominant one (can contribute 90% of total uncertainty).

VBF H→$\tau\tau$

Submittend to PRD (arXiv: 1811.08856)

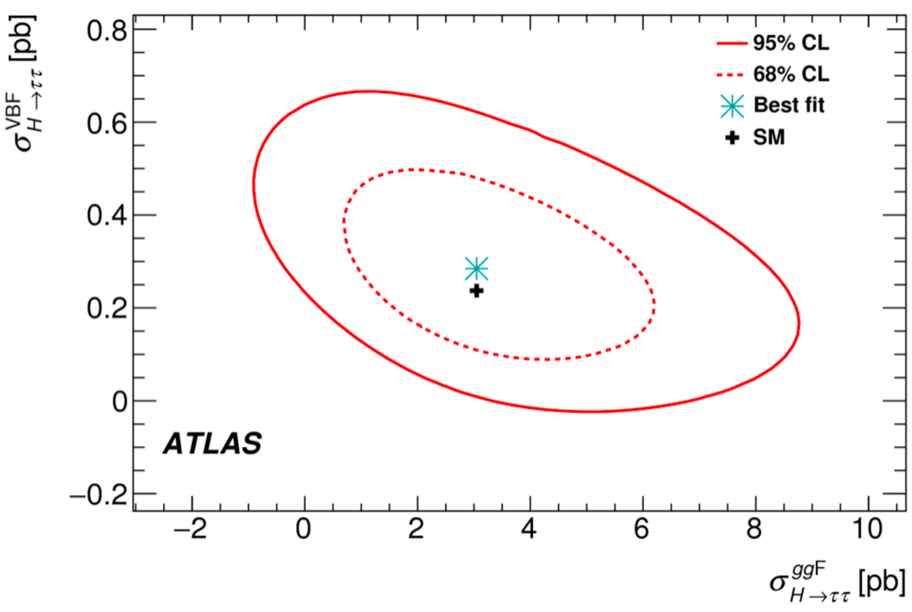

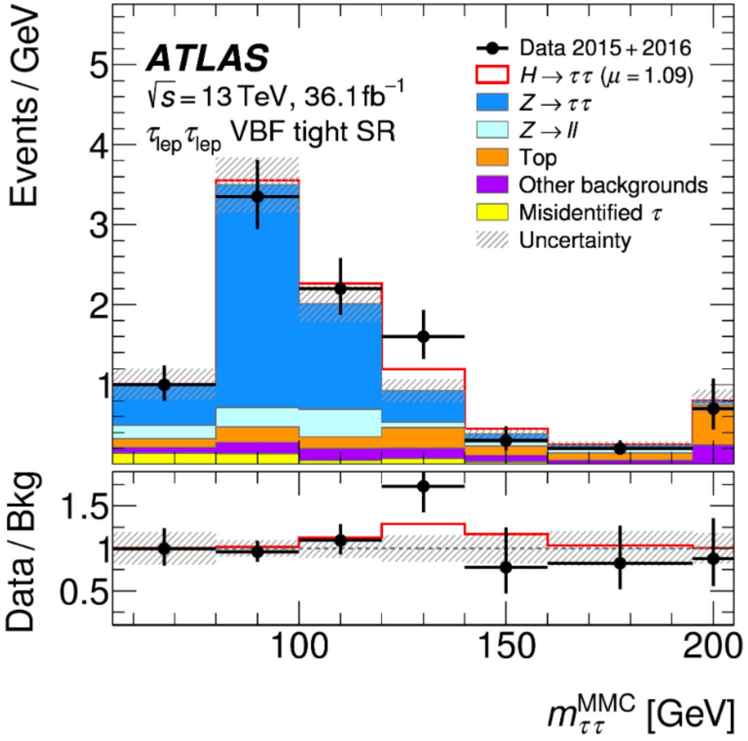

Process	Particle-level selection	σ [pb]	σ^{SM} [pb]
ggF	$N_{jets} \geq 1,\ 60 < p_T^H < 120\,\text{GeV},\ \lvert y_H\rvert < 2.5$	$1.79 \pm 0.53\,(\text{stat.}) \pm 0.74\,(\text{syst.})$	0.40 ± 0.05
ggF	$N_{jets} \geq 1,\ p_T^H > 120\,\text{GeV},\ \lvert y_H\rvert < 2.5$	$0.12 \pm 0.05\,(\text{stat.}) \pm 0.05\,(\text{syst.})$	0.14 ± 0.03
VBF	$\lvert y_H\rvert < 2.5$	$0.25 \pm 0.08\,(\text{stat.}) \pm 0.08\,(\text{syst.})$	0.22 ± 0.01

- For the VBF H→$\tau\tau$, the observed signal strength is slightly higher than the SM prediction.

VBF H→*bb*

- VBF H→*bb* analysis is divided into two categories (tagging or non-tagging photon)
- The tagging of one photon is efficient to suppress QCD background.

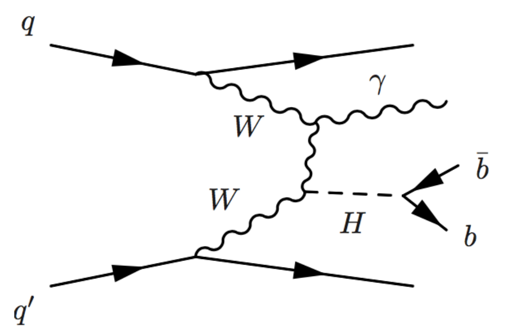

CERN-EP-2018-140

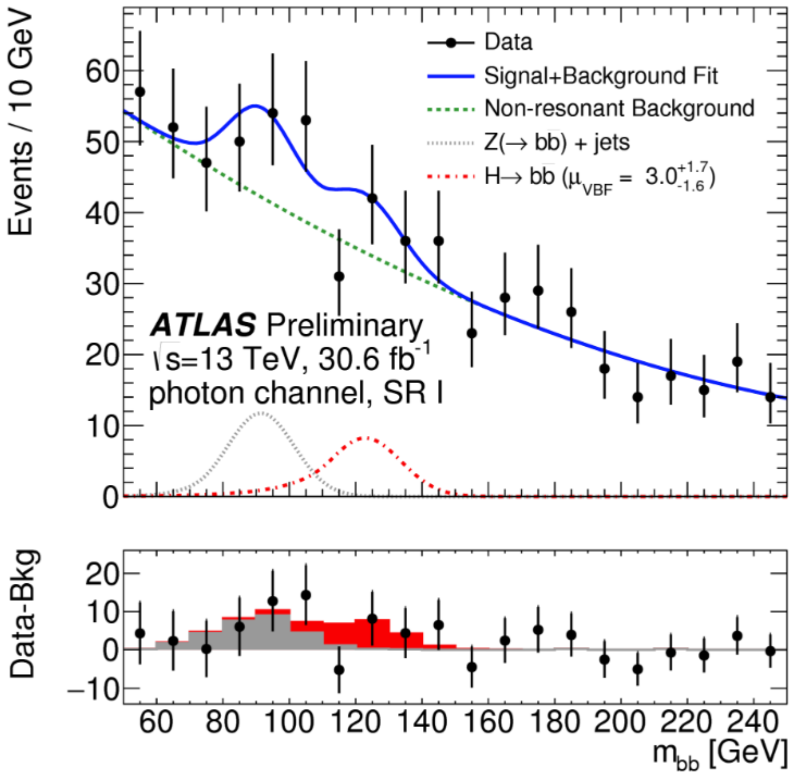

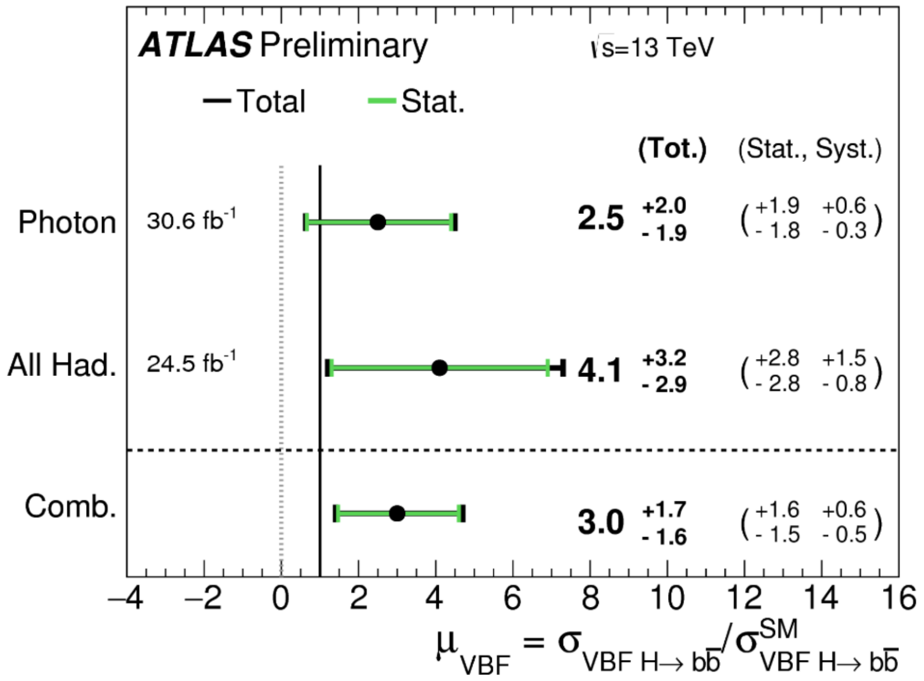

➢ **The observed signal strength for VBF H→*bb* is ~3xSM, which is still consistent with SM within the error bar.**

ATLAS VBF H→*WW**

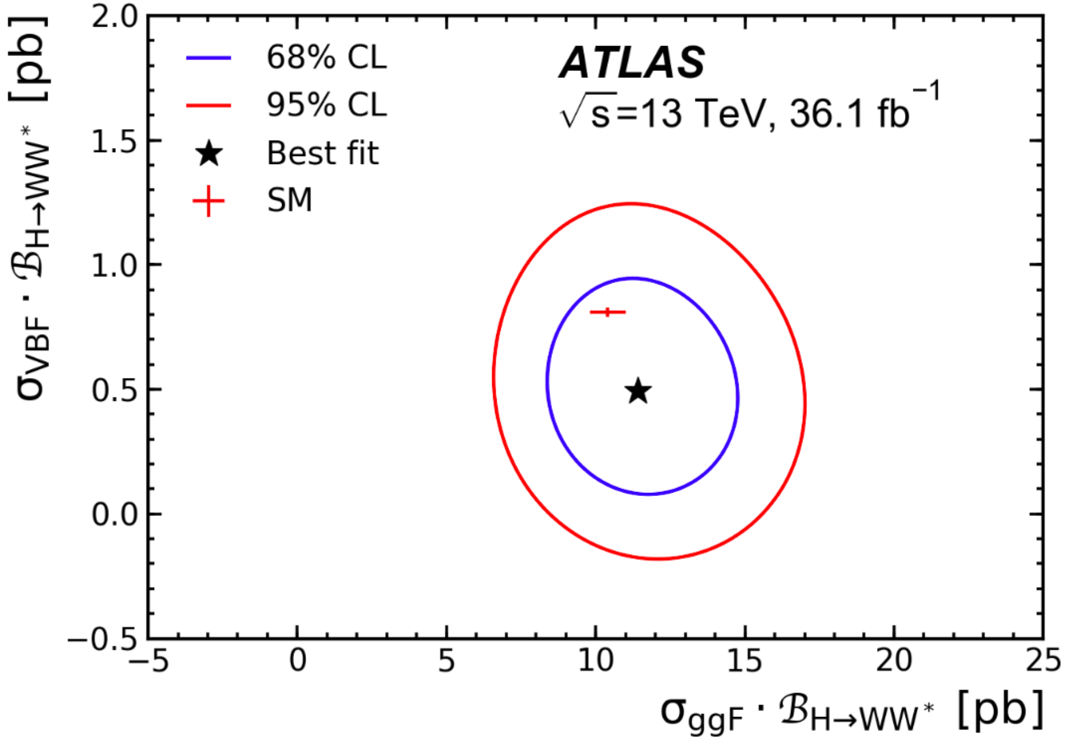

Source	$\Delta\sigma_{\mathrm{ggF}} \cdot \mathcal{B}_{H\to WW^*}$ [%]	$\Delta\sigma_{\mathrm{VBF}} \cdot \mathcal{B}_{H\to WW^*}$ [%]
Data statistics	10	46
CR statistics	7	9
MC statistics	6	21
Theoretical uncertainties	10	19
ggF signal	5	13
VBF signal	<1	4
WW	6	12
Top-quark	5	5
Experimental uncertainties	8	9
b-tagging	4	6
Modelling of pile-up	5	2
Jet	2	2
Lepton	3	<1
Misidentified leptons	6	9
Luminosity	3	3
TOTAL	18	57

Submitted to PLB (arxiv:1808.09054)

$$\mu_{\mathrm{ggF}} = 1.10^{+0.10}_{-0.09}(\mathrm{stat.})^{+0.13}_{-0.11}(\mathrm{theo\ syst.})^{+0.14}_{-0.13}(\mathrm{exp\ syst.}) = 1.10^{+0.21}_{-0.20}$$

$$\mu_{\mathrm{VBF}} = 0.62^{+0.29}_{-0.27}(\mathrm{stat.})^{+0.12}_{-0.13}(\mathrm{theo\ syst.}) \pm 0.15(\mathrm{exp\ syst.}) = 0.62^{+0.36}_{-0.35}$$

VBF is around 0.6xSM prediction which is still consistent with SM prediction considering the large statistical uncertainty.

correlation to m_H

- the used variables should not be correlated to $m_{\gamma\gamma}$

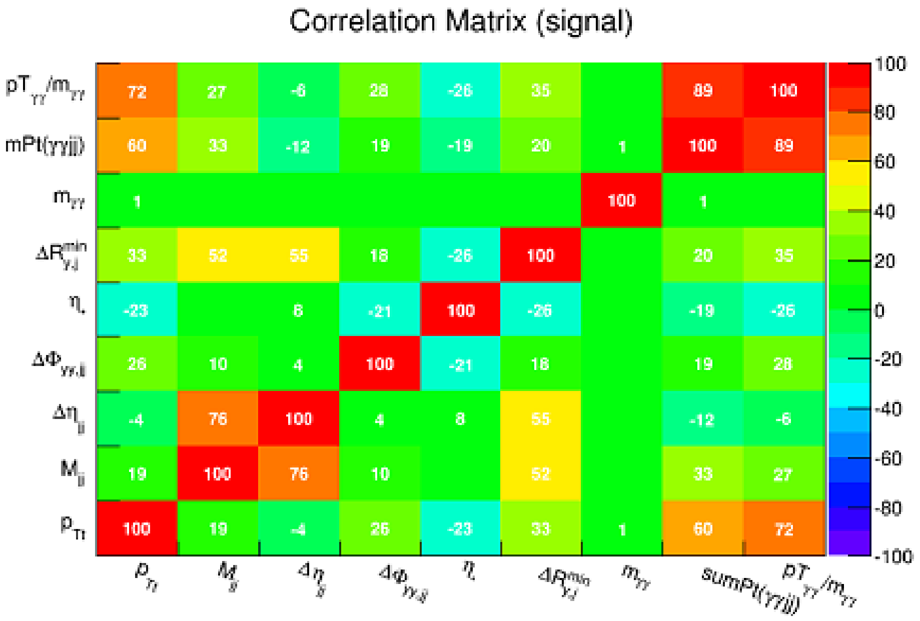

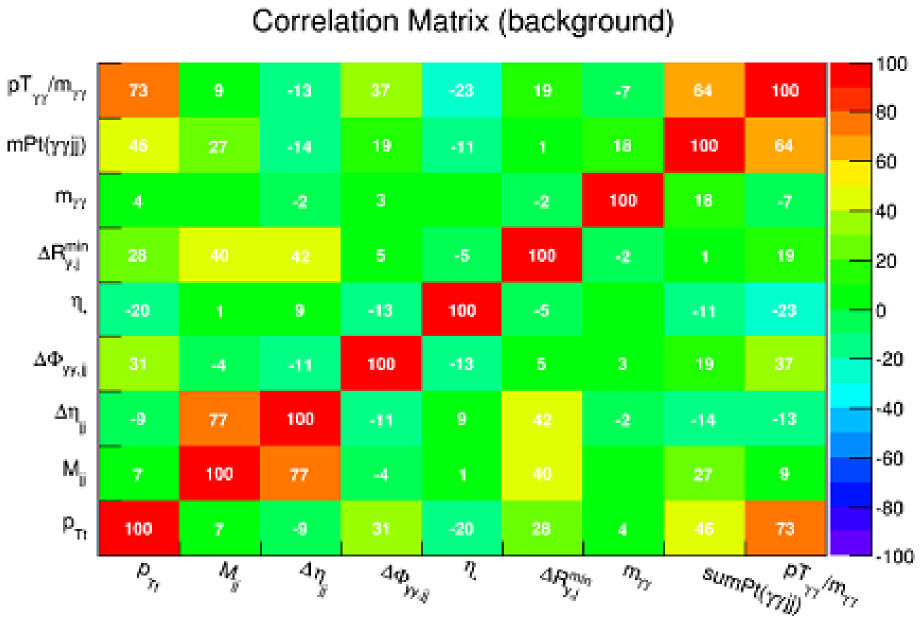

CMS VBF H->γγ strategy

Events produced via the VBF mechanism features two jets in the final state separated by a large rapidity gap. A multivariate discriminant is trained to tag the VBF jets kinematics, considering as background the production process of ggH + jets, and is given as input to an additional "combined" multivariate classifier along with the score of the photon identification MVA, the diphoton BDT score, and the ratio $p_{T\gamma\gamma}/m_{\gamma\gamma}$. Figure 7 (left) shows the transformed score of the combined multivariate classifier for data in the mass side-band region 105-115 GeV and 135-145 GeV, along with the predicted VBF and ggH distributions. The classifier score has been transformed such that the signal events from the VBF production mode has a uniform, flat, distribution. A validation of the score of the combined multivariate classifier obtained in $Z \to e^+e^-$ + jets events, where the electrons are reconstructed as photons and at least two jets satisfy the requirements listed below to enter the VBF category, is shown in Fig. 7 (right) for data and simulation.

Selections:

- one jet with $p_T > 40$ GeV and one with $p_T > 30$ GeV, both with $|\eta| < 4.7$ and width a tight requirement on the pileup jet identification;
- the invariant mass of the two jets $m_{jj} > 250$ GeV;
- the combined multivariate discriminant greater than 0.43.

- leading photon $p_T > m_{\gamma\gamma}/3$, sub-leading photon $p_T > m_{\gamma\gamma}/4$;
- photon ID BDT score greater than -0.2, in order to provide additional rejection against background events whose kinematics yield a high diphoton BDT score despite one reconstructed photon with a relatively low ID score;

- ➢ BDT training :
  - VBF Higgs vs ggH+jets
  - Divided into 3 cats.
- ➢ Validated with Z->ee events

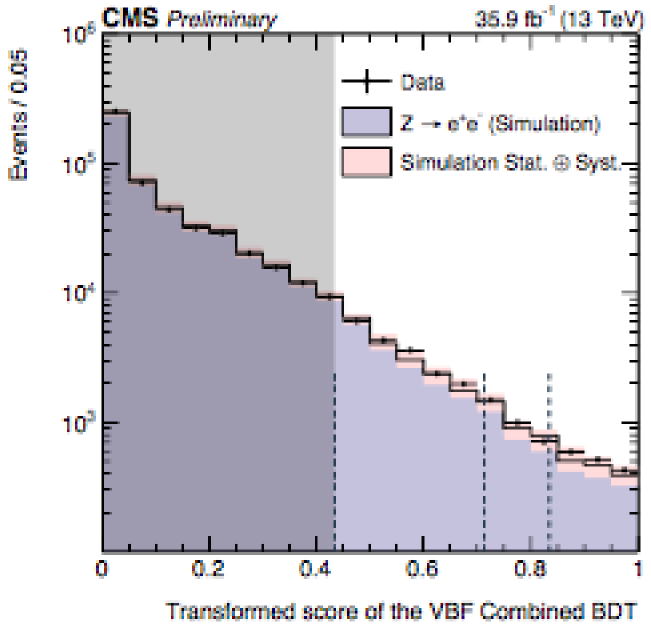

CMS VBF H->γγ

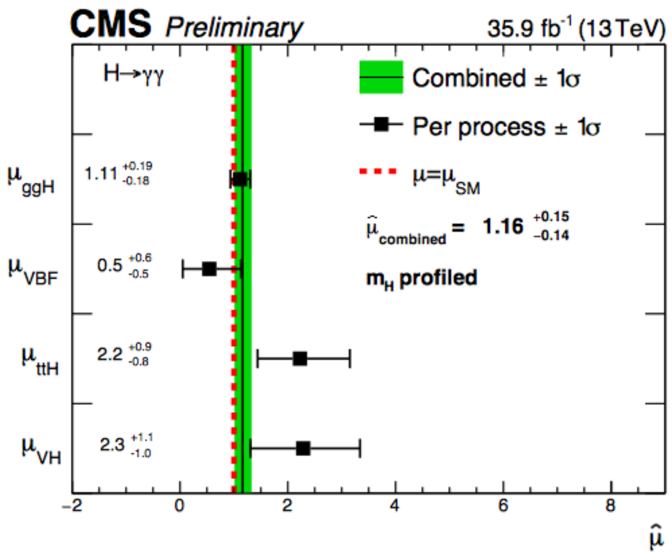

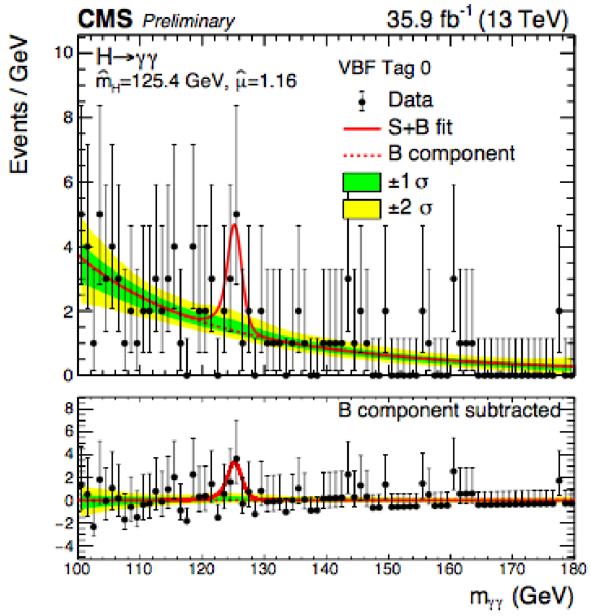

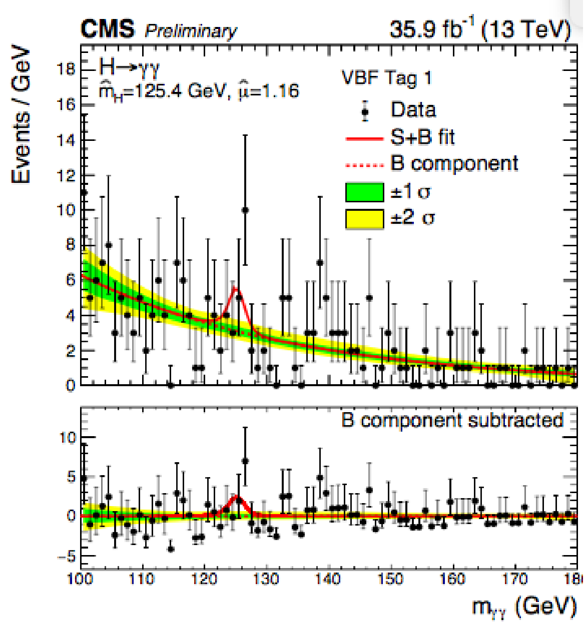

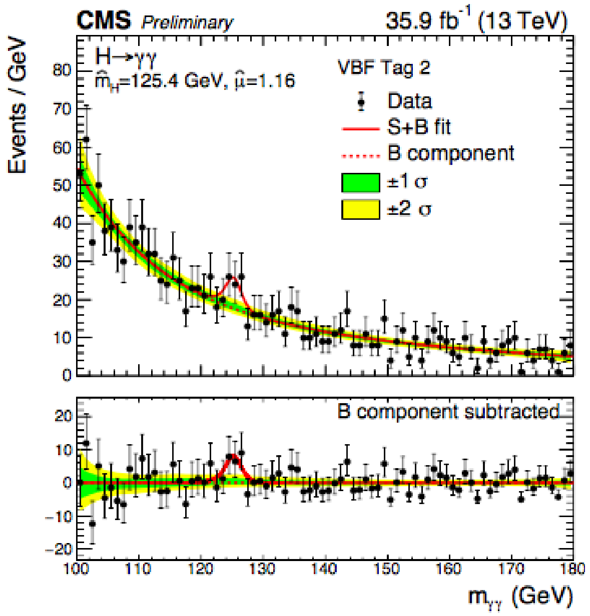

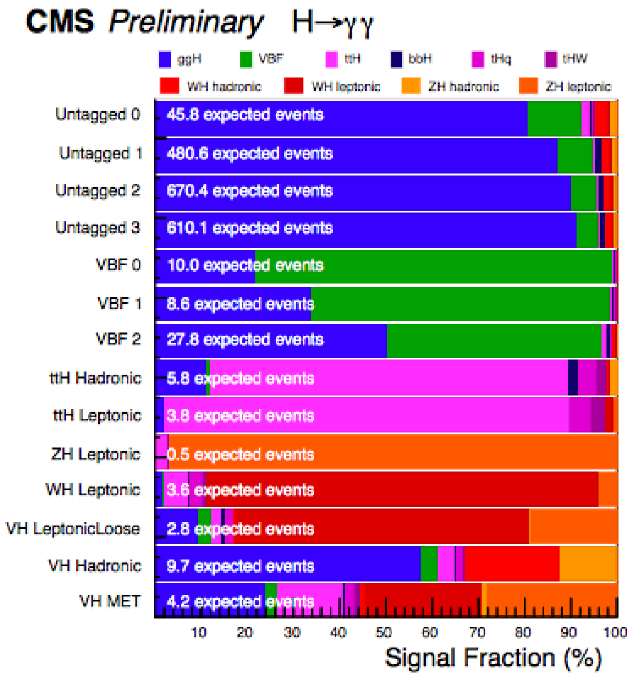

Observed (expected) Significance = 1.1σ/1.9σ

CMS VBF H->ZZ

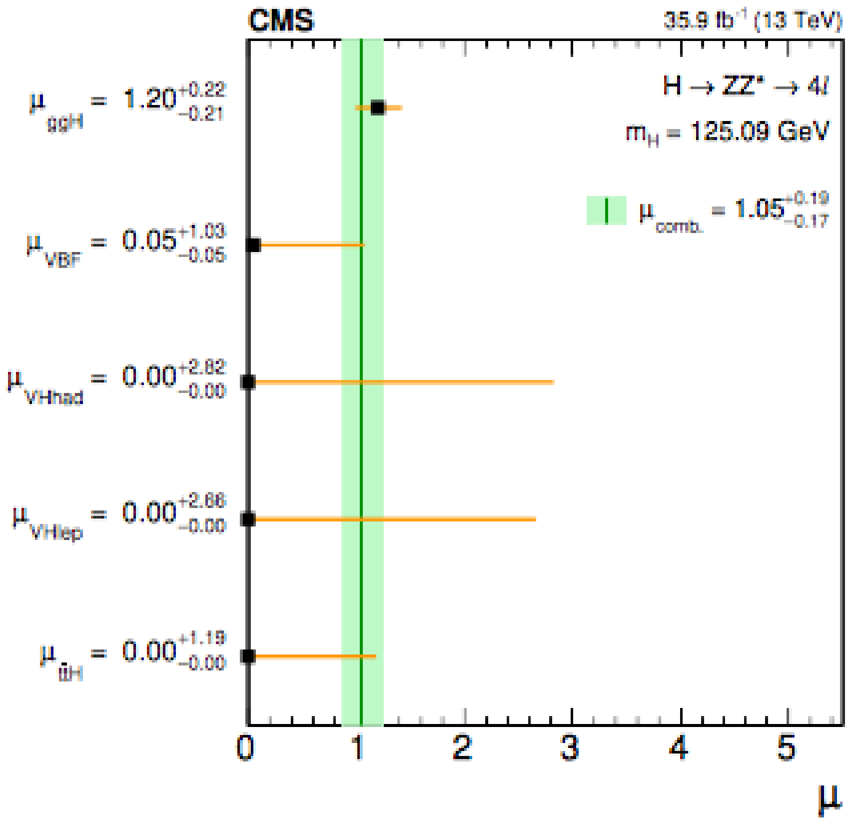

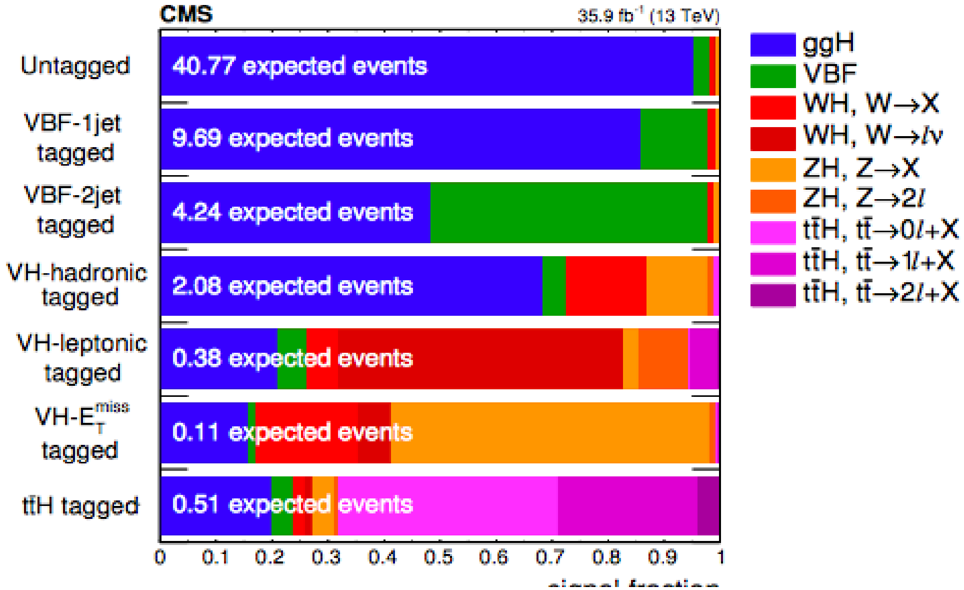

	Event category							
	Untagged	VBF-1j	VBF-2j	VH-hadr.	VH-lept.	VH-E_T^{miss}	$t\bar{t}H$	Inclusive
$q\bar{q} \rightarrow ZZ$	19.18	2.00	0.25	0.30	0.27	0.01	0.01	22.01
$gg \rightarrow ZZ$	1.67	0.31	0.05	0.02	0.04	0.01	<0.0	2.09
Z+X	10.79	0.88	0.78	0.31	0.17	0.30	0.27	13.52
Sum of backgrounds	31.64	3.18	1.08	0.63	0.49	0.32	0.28	37.62
uncertainties	$^{+4.30}_{-3.42}$	$^{+0.37}_{-0.32}$	$^{+0.29}_{-0.21}$	$^{+0.13}_{-0.09}$	$^{+0.07}_{-0.07}$	$^{+0.14}_{-0.11}$	$^{+0.09}_{-0.07}$	$^{+5.19}_{-4.18}$
$gg \rightarrow H$	38.78	8.31	2.04	1.41	0.08	0.02	0.10	50.74
VBF	1.08	1.14	2.09	0.09	0.02	<0.01	0.02	4.44
WH	0.43	0.14	0.05	0.30	0.21	0.03	0.02	1.18
ZH	0.41	0.11	0.04	0.24	0.04	0.07	0.02	0.93
$t\bar{t}H$	0.08	<0.01	0.02	0.03	0.02	<0.01	0.35	0.50
Signal	40.77	9.69	4.24	2.08	0.38	0.11	0.51	57.79
uncertainties	$^{+3.69}_{-3.62}$	$^{+1.13}_{-1.17}$	$^{+0.55}_{-0.55}$	$^{+0.23}_{-0.23}$	$^{+0.03}_{-0.03}$	$^{+0.01}_{-0.02}$	$^{+0.06}_{-0.06}$	$^{+4.89}_{-4.80}$
Total expected	72.41	12.88	5.32	2.71	0.86	0.43	0.79	95.41
uncertainties	$^{+7.35}_{-6.27}$	$^{+1.25}_{-1.21}$	$^{+0.78}_{-0.65}$	$^{+0.34}_{-0.28}$	$^{+0.10}_{-0.09}$	$^{+0.15}_{-0.12}$	$^{+0.14}_{-0.12}$	$^{+9.86}_{-8.32}$
Observed	73	13	4	2	1	1	0	94

Table 2. The numbers of expected background and signal events and the number of observed candidate events after the full selection, for each event category, for the mass range $118 < m_{4\ell} < 130$ GeV. The yields are given for the different production modes. The signal and ZZ backgrounds yields are estimated from simulation, while the Z+X yield is estimated from data.